8.5

ALGORITHMS FOR DROP SIZE DISTRIBUTION RETRIEVAL FROM POLARIMETRIC RADAR MEASUREMENTS

V. Chandrasekar[1]*, Eugenio Gorgucci[2#], V. N. Bringi[1]
[1] Colorado State University, Fort Collins, Colorado
[2] Istituto di Scienze dell'Atmosfera e del Clima (CNR), Rome, Italy

1. INTRODUCTION

Ever since the introduction of differential reflectivity (Z_{dr}) measurement, one of the long-standing goals of polarimetric radar has been the estimation of the raindrop size distribution (DSD). Seliga and Bringi (1976) showed that Z_{dr}, for an exponential DSD, is directly related to the median volume diameter (D_o). Careful intercomparisons between radar measurements of Z_{dr} and D_o derived from surface disdrometers and airborne imaging probes have shown that D_o can be estimated to an accuracy of about 10-15% (see, for example, Aydin et al., 1987; Bringi et al., 1998). A general gamma distribution model was suggested by Ulbrich (1983) to characterize the natural variation of the DSD. The specific differential propagation phase (K_{dp}) is a forward scatter measurement whereas Z_{dr} is a backscatter measurement. The weighting of the DSD by Z_{dr} and K_{dp} is controlled by the variation of mean raindrop shape with size. A combination of the three radar measurements (Z_h, Z_{dr} and K_{dp}) can be utilized to estimate the DSD, specifically a parametric form of the DSD such as the gamma DSD. This paper presents algorithms for the estimation of parameters of a gamma DSD from polarimetric radar measurements at various frequency bands.

2. RAINDROP SIZE DISTRIBUTION

The raindrop size distribution describes the probability density/distribution function of raindrop sizes. In practice, the normalized histogram of raindrop sizes (normalized with respect to the total number of observed raindrops) converges to the probability density function of raindrop sizes. A gamma distribution model can adequately describe many of the natural variations in the shape of the raindrop size distribution (Ulbrich, 1983). The gamma raindrop size distribution can be expressed as (Chandrasekar and Bringi, 1986),

$$N(D) = n_c f_D(D) \qquad (m^{-3}\, mm^{-1}) \qquad (1)$$

where $N(D)$ is the number of raindrops per unit volume per unit size interval (D to $D+\Delta D$), n_c is the number concentration and $f_D(D)$ is the probability density function (pdf). When $f_D(D)$ is of the gamma form it is given by,

$$f_D(D) = \frac{\Lambda^{\mu+1}}{\Gamma(\mu+1)} e^{-\Lambda D} D^{\mu}, \qquad \mu > -1 \qquad (2)$$

where Λ and μ are the parameters of the gamma pdf. Any other gamma form such as the one introduced by Ulbrich (1983),

$$N(D) = N_0 D^{\mu} e^{-\Lambda D} \qquad (3)$$

can be derived from this fundamental notion of raindrop size distribution. It must be noted that any function used to describe $N(D)$ when integrated over D must yield the total number concentration, to qualify as a DSD function. This property is a direct consequence of the fundamental result that any probability density function must integrate to unity. The relation between D_o, μ and Λ is given by

$$\Lambda D_o \cong 3.67 + \mu \qquad (4)$$

Similarly, a mass-weighted mean diameter D_m can be defined as

$$D_m = \frac{E(D^4)}{E(D^3)} \qquad (5)$$

where E stands for the expected value. Using (4), $f_D(D)$, the gamma pdf described by (2), can be written in terms of D_0 and μ as,

$$f_D(D) = \frac{(3.67+\mu)^{\mu+1}}{\Gamma(\mu+1)D_0} \cdot \left(\frac{D}{D_0}\right)^{\mu} e^{-\left[(3.67+\mu)\frac{D}{D_0}\right]} \qquad (6)$$

The above form makes the normalized diameter (D/D_0) as the variable rather than D. Several measurables such as water content (W) and rainfall rate (R) can be expressed in terms of the DSD as,

$$W = \frac{\pi}{6} \rho_w n_c E(D^3) \qquad (7)$$

and

$$R = \frac{\pi}{6} n_c E[\upsilon(D) D^3] \qquad (8a)$$

where R is the still-air rainfall rate and $\upsilon(D)$ is the terminal velocity of raindrops (Gunn and Kinzer, 1949). The conventional unit of rainfall rate is $mm\ h^{-1}$. Converting to this unit, rainfall rate is expressed as,

$$R = 0.6\pi \times 10^{-3} n_c \cdot E[\upsilon(D) D^3] \qquad (mm\, h^{-1}) \qquad (8b)$$

where n_c is in m^{-3}, v(D) in m s^{-1} and D in mm.

In order to compare the pdf of D (or, $f_D(D)$) in the presence of varying water contents, the concept of scaling the DSD has been used by several authors (Sekhon and Srivastava, 1971; Willis, 1984; and Testud et al., 2000). The corresponding form of $N(D)$ can be expressed as,

**Corresponding author address*: V. Chandrasekar, Colorado State University, Fort Collins, CO. 80523-1373; e-mail: chandra@engr.colostate.edu
[#]Eugenio Gorgucci, Istituto di Scienze dell'Atmosfera e del Clima (CNR), Area di Ricerca Roma-Tor Vergata, Via del Fosso del Cavaliere, 100-00133 Rome, Italy; e-mail:gorgucci@radar.ifa.rm.cnr.it

$$N(D) = N_w f(\mu)\left(\frac{D}{D_0}\right)^{\mu} \exp\left[-(3.67+\mu)\frac{D}{D_0}\right] \quad (9)$$

where N_w is the scaled version of N_0 defined in (3),

$$N_w = \frac{N_0}{f(\mu)} D_0^{\mu} \quad (10a)$$

and

$$f(\mu) = \frac{6}{(3.67)^4} \cdot \frac{(3.67+\mu)^{\mu+4}}{\Gamma(\mu+4)} \quad (10b)$$

with $f(0)=1$ and $f(\mu)$ is a unit less function of μ. One interpretation of N_w is that it is the intercept of an equivalent exponential distribution with the same water content and D_0 as the gamma DSD. (Bringi and Chandrasekar, 2001). Thus N_w, D_0 and μ form the three parameters of the gamma DSD.

3. RAINDROP SHAPE AND IMPLICATION FOR POLARIMETRIC RADAR MEASUREMENTS

The equilibrium shape of raindrops is determined by a balance of hydrostatic, surface tension and aerodynamic forces. The commonly used model for raindrops assumes oblate spheroidal shapes, with the axis ratio b/a, where b and a are the semi-minor and the semi-major axis lengths, respectively. Pruppacher and Beard (1970) give a simple model for the axis ratio (r) based on a linear fit to wind tunnel data as,

$$r = 1.03 - 0.062D; \qquad 1 \le D \le 9\ mm. \quad (11)$$

Rotating linear polarization data in heavy rain (Hendry et al., 1987) has indicated that raindrops fall with the mean orientation of their symmetry axis in the vertical direction. The large swing in the crosspolar power in their data implies a high degree of orientation of drops with the standard deviation of canting angles estimated to be around 6° assuming a Gaussian model. It is reasonable to assume that the standard deviation of canting angles is in the range 5-10° (Bringi and Chandrasekar, 2001).

3.1 Differential Reflectivity

The differential reflectivity can be written as (Seliga and Bringi, 1976),

$$10\log_{10}\frac{E[\sigma_{hh}(D)]}{E[\sigma_{vv}(D)]} = 10\log_{10}(\xi_{dr}) \quad (12)$$

where the symbol E represents expectation and σ_{hh} and σ_{vv} are the cross sections at horizontal and vertical polarizations, respectively.

Seliga and Bringi (1976) showed that for an exponential distribution and axis ratio given by (11), Z_{dr} can be expressed as a function of the median volume diameter D_o. This microphysical link between a radar measurement and a parameter of the DSD is important. More fundamentally, ξ_{dr}^{-1} may be related to the reflectivity factor weighted mean of $r^{7/3}$ (Jameson, 1985). For a more general gamma form an approximate power law fit can be derived assuming $-1 \le \mu \le 5$, $0.5 < D_o < 2.5\ mm$, and N_w chosen to be consistent with thunderstorm rain rates. Using the fit recommended by Andsager et al. (1999) for the Beard and Chuang (1987) equilibrium shapes power law fits to D_0 and D_m can be derived as,

$$D_0 = 1.619(Z_{dr})^{0.485} \qquad (mm) \quad (13a)$$

$$D_m = 1.529(Z_{dr})^{0.467} \qquad (mm) \quad (13b)$$

where Z_{dr} is in decibels and the fits are valid at S band frequency (near 3 GHz, Bringi and Chandrasekar, 2001).

3.2 Specific Differential Phase

The relation between specific differential phase (K_{dp}) and the water content and raindrop axis ratio was described by Jameson (1985).

K_{dp} can be related to the water content as (Bringi and Chandrasekar, 2001)

$$K_{dp} = \left(\frac{180}{\lambda}\right)\cdot 10^{-3}\cdot c\cdot W(1-\overline{r_m}) \quad (\text{deg. } km^{-1}) \quad (18)$$

where $c \cong 3.75$ is both dimensionless and independent of wavelength. This result links the specific differential phase with parameters of the DSD. If the equilibrium axis ratio model given in (11) is used in (18) then K_{dp} is given by,

$$K_{dp} = \left(\frac{180}{\lambda}\right)\cdot 10^{-3}\cdot c\cdot W(0.062)D_m(\text{deg. } km^{-1}) \quad (19)$$

Thus K_{dp} is related to the product of D_m and water content. Though the above result was obtained using the Rayleigh-Gans approximation, it is valid up to 13 GHz (Bringi and Chandrasekar, 2001).

3.3 Mean Raindrop Shape Derived From Polarimetric Radar Measurements

Gorgucci et al. (2000) assumed a simple linear model for axis ratio versus size of the form,

$$r = 1 - \beta D \quad (20)$$

and derived radar-based estimators of β.

It was shown in section 3a that ξ_{dr}^{-1} is related to the reflectivity weighted axis ratio. Similar dependence on K_{dp} can be derived from (18). Let $p(r)$ be the probability density function of the axis ratio for a given diameter. The expression for K_{dp} can be generalized as (Bringi and Chandrasekar, 2001),

$$K_{dp} = \frac{2\pi c'}{k_0}\int D^3 N(D)\int (1-r)p(r)\,dr\,dD \quad (21)$$

$$= \frac{2\pi c'}{k_0}\int D^3 N(D)[1-E(r)]\,dD \quad (22)$$

where $E(r)$ is the mean value of r, and c' is a constant. The functional dependence of $E(r)$ versus D may be modeled as in (20). Using the linear model in (20), Gorgucci et al. (2000) showed the variations of Z_{dr} and K_{dp} with respect to β, and in turn derived an estimator for β based on polarimetric radar measurements. This can be used subsequently in algorithms relating Z_{dr} and K_{dp} to the parameters of the DSD, which gives rise to a methodology for estimating the gamma DSD parameters based on radar measurements.

4. ESTIMATORS OF THE GAMMA DSD PARAMETERS

Seliga and Bringi (1976) showed that for an exponential distribution, the two parameters of the DSD, namely N_w and D_0, can be estimated using Z_{dr} and Z_h. They used a two-step procedure where they estimated D_0 using an equilibrium raindrop shape model and subsequently used that in the expression for Z_h to estimate N_w. This procedure can essentially be applied for a gamma DSD, and generalized to account for raindrop oscillations using the linear model in (20). The procedure for estimating the gamma DSD parameters is as follows: first estimate β using the algorithm described by Gorgucci et al. (2000), and subsequently, estimate $\hat{D}_o$, N_w and μ recognizing the prevailing β value. Using simulations, an estimator for $\hat{D}_0$ can be derived as

$$\hat{D}_0 = a_1 Z_h^{b_1} (\xi_{dr})^{c_1} \quad (23)$$

These coefficients for S-band are

$$a_1 = 0.56,\ b_1 = 0.064,\ c_1 = 0.024\beta^{-1.42} \quad (24)$$

Similar estimates can be derived for C and X band as with the corresponding coefficients are given in table 1.

Coefficients	a_1	b_1	c_1
S	0.56	0.064	$0.024\,\beta^{-1.42}$
C	0.526	0.0973	$0.0118\,\beta^{-1.31}$
X	$0.195\,\beta^{-0.55}$	0.0498	$0.0344\,\beta^{-0.471}$

Table 1 The coefficients of D_o estimate parameters at S, C, and X band

Simulations can also be utilized to evaluate the performance of the estimator of D_0 in (23). Figure 1 shows a scatter plot of $\hat{D}_0$ versus true D_0 at S band for widely varying β and gamma DSD parameters as given by (23). Quantitative analysis of the scatter gives a correlation coefficient of 0.963. It can be seen from Fig. 1 that D_0 is estimated fairly well with negligible bias over a wide range. Figure 2 shows the normalized standard deviation (NSD) of $\hat{D}_0$ as a function of D_0. Figure 2 shows that D_0 can be estimated to an accuracy of about 10% when D_0 > 1 mm. The corresponding parameters at C and X band are as follows. The correlation coefficients are 0.93 and 0.95, whereas the normalized standard errors are 15% and 13% respectively.

4.1 *Estimation of N_w*

Once D_0 is estimated, N_w can be easily estimated using one of the moments of the DSD such as Z_h or K_{dp}. For example, Z_h can be written in terms of the gamma DSD parameters as,

$$\frac{Z_h}{N_w} = F_z(\mu)\, D_0^{\,7} \quad (25)$$

Thus it can be seen that N_w can be estimated in terms of D_0. However, the estimate of D_0 can be obtained in terms of Z_h and Z_{dr} (or K_{dp} and Z_{dr}). Therefore, a direct estimate of N_w can be pursued of the form,

$$\log_{10}(N_w) = a_2\, Z_h^{\,b_2}\, \xi_{dr}^{\,c_2} \quad (26)$$

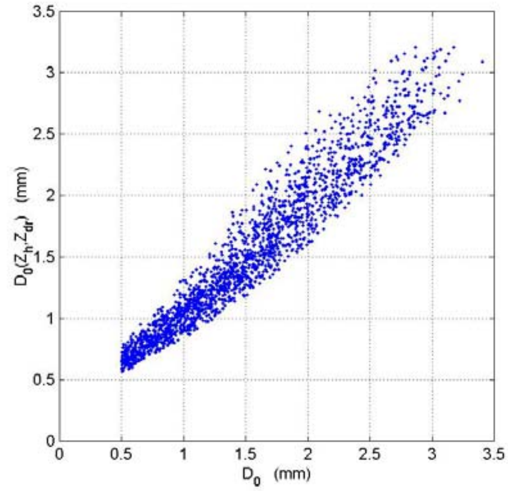

Figure 1. Scatterplot of $D_0(Z_h, Z_{dr})$ versus the true value of D_0 for widely varying RSD, at S band.

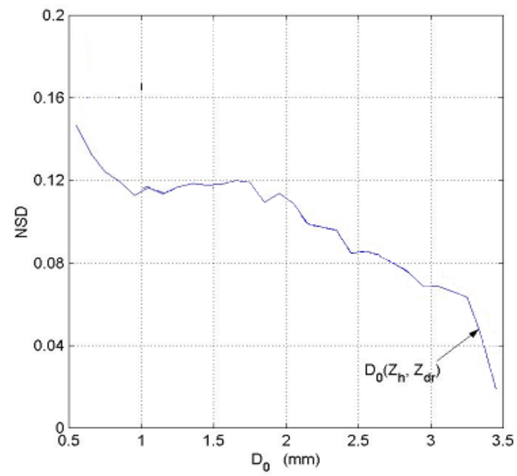

Figure 2. Normalized standard deviation (NSD) in the estimates of D_0 as a function of the true value of D_0 at S band.

The variability of a_2, b_2, c_2 can be parameterized in terms of β at S band as

$$a_2 = 3.29,\ b2 = 0.058,\ c2 = -0.023\beta^{-1.389} \quad (27)$$

In summary, the estimator for N_w is obtained as follows. Using Z_h, Z_{dr} and K_{dp} first estimate β as given in (26). Subsequently, calculate the coefficients in (27) and use in (26) to estimate N_w. Figure 3 shows a scatter plot of $\log_{10}\hat{N}_w$ versus true $\log_{10}$ N_w, where $\log_{10}\hat{N}_w$ is estimated using (26). It can be seen from Fig. 3 that $\log_{10}\hat{N}_w$ is estimated fairly well. Quantitative analysis of the scatter yields a correlation coefficient of 0.831. Fig. 3 shows the NSD of $\log_{10}\hat{N}_w$ as a function of $\log_{10}\hat{N}_w$. It can be seen, from Fig. 4, that $\log_{10} N_w$ is estimated to a normalized standard deviation of better than 7% when $\log_{10} N_w$ > 3.5. Note that due to the wide variability of N_w, $\log_{10} N_w$ is the preferred scale of comparison (similar to dB scale for reflectivity). At C and X bands the parameterization for N_w can be obtained in a similar manner and the results are summarized in table 2.

Coefficients	a_2	b_2	c_2
S	3.29	0.058	$-0.023\ \beta^{-1.389}$
C	$3.62\ \beta^{-0.0622}$	0.054	$-0.03\ \beta^{-1.12}$
X	2.97	0.072	$-0.0294\ \beta^{-1.26}$

Table 2 One coefficients of N_w estimate parameters at S, C, and X band.

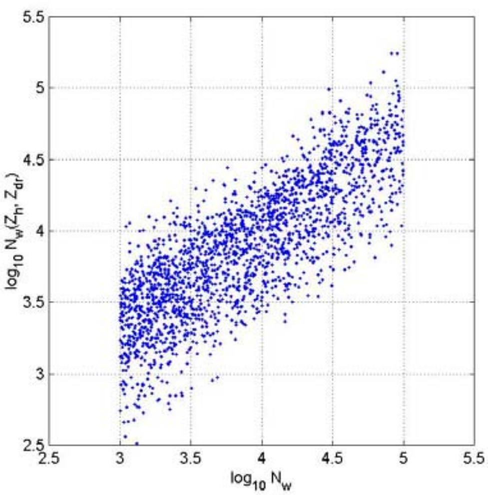

Figure 3. Scatterplot of $\log_{10} N_w(Z_h, Z_{dr})$ versus the true value of the $\log_{10} N_w$ for widely varying RSD at S band.

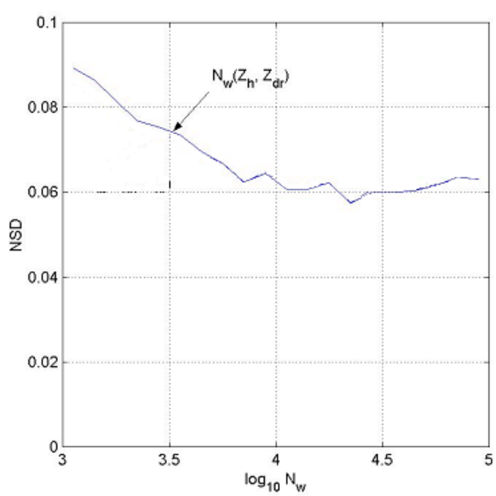

Figure 4. Normalized standard deviation in the estimates of $\log_{10} N_w$, as a function of $\log_{10} N_w$ at S band.

4.2 Parameterization of μ

The parameter μ describes the overall shape of the distribution. Once D_0 is estimated, μ can be estimated from the following parameterization which was constructed empirically as,

$$\hat{\mu} = \frac{a_5\, D_0^{\,b_5}}{(\xi_{dr} - 1)} - c_5\, (\xi_{dr})^{d_5} \qquad (28)$$

The variability of a_5, b_5, c_5 and d_5 can be parameterized in terms of β as

$$a_5 = 200\ \beta^{1.89} \qquad (29a)$$

$$b_5 = 2.23\,\beta^{0.039} \qquad (29b)$$

$$c_5 = 3.16\ \beta^{-0.046} \qquad (29c)$$

$$d_5 = 0.374\,\beta^{-0.355} \qquad (29d)$$

D_0 calculated from (23) can be utilized in (28) to estimate μ. However, in practice D_0 has to be estimated using Z_h, Z_{dr} and K_{dp}. Estimating μ under such conditions will result in large errors than that. Estimating μ accurately under practical conditions, especially in the presence of measurement errors is very difficult using the procedures discussed here.

5. IMPACT OF MEASUREMENT ERROR ON THE ESTIMATES OF D_0 AND N_W.

Estimators of D_o use measurements of Z_h, Z_{dr}, and K_{dp}. Any error in the measurement of these three parameters will directly translate into errors in the estimates of D_o and N_w. The three measurements Z_h, Z_{dr}, and K_{dp} have completely different error structures.

The Z_h is based on absolute power measurement and has a typical accuracy of 1 dB. The Z_{dr} is a relative power measurement which can be estimated to an accuracy of about 0.2 dB. K_{dp} is the slope of the range profile of the differential propagation phase Φ_{dp}, which can be estimated to an accuracy of a few degrees. The subsequent estimate of K_{dp} depends on the procedure used to compute the range derivative of Φ_{dp} such as a simple finite-difference scheme or a least squares fit. Using a least squares estimate of the Φ_{dp} profile, the standard deviation of K_{dp} can be expressed as (Gorgucci et al. 1999),

$$\sigma(K_{dp}) = \sqrt{3}\ \frac{\sigma(\Phi_{dp})}{N\Delta r}\sqrt{\frac{N}{(N-1)(N+1)}}, \qquad (30)$$

where Δr is the range resolution of the Φ_{dp} estimate and *N* is the number of range samples along the path. For a typical 150 m range spacing, and with 2.5° accuracy of Φ_{dp}, K_{dp} can be estimated over a path of 3 km, with a standard error of 0.32° km^{-1}.

The measurement errors of Z_h, Z_{dr}, and K_{dp} are nearly independent. In the following, simulations are used to quantify the error structure of the estimates of D_0 and N_w.

The normalized standard deviation in the estimates of D_0 and N_w including the effect of measurement error are evaluated and shown in Figs. 5 and 6, respectively. Fig. 5 shows the NSD in the estimates of D_0. Comparing Fig. 5 to Fig. 2 it can be seen that in general, there is about a 10% increase in the NSD of D_0 estimate due to measurement error. The NSD of the N_w estimates in the presence of measurement errors, are shown in Fig. 6. Again comparing these to the NSD computations without measurement error (Fig. 4), a 4% to 16%

increase is noted depending on the value of N_w. Thus, D_0 and N_w can be estimated fairly well from radar measurements at least for convective rainfall with $R \geq$ 5-10 mm h^{-1}. These errors can be further reduced using other techniques such as spatial averaging whenever possible. The following section presents evaluation of the algorithms developed here using disdrometer observations.

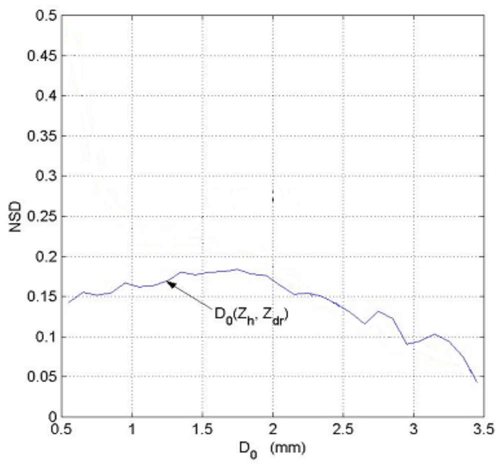

Figure 5. Normalized standard deviation in the estimates of D_0 as a function of D_0 in the presence of radar measurement errors at S band.

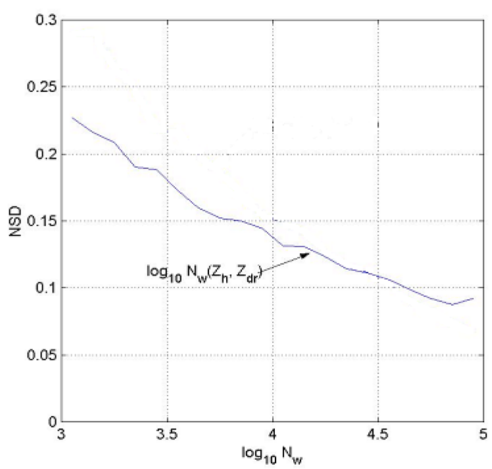

Figure 6. Normalized standard deviation (NSD) in the estimates of $\log_{10} N_w$ as a function of $\log_{10} N_w$ in the presence of radar measurement errors at S band.

6. EVALUATION OF THE ALGORITHMS USING DISDROMETER DATA

The algorithms developed in this paper to estimate D_o and N_w are applied to data collected with a J-W impact disdrometer (Joss and Waldvogel 1967) during a rainfall season (covering about three months) from Darwin (Australia). This data set was collected by the Bureau of Meteorology Research Center (BMRC) and includes a variety of rainfall types from a tropical regime with rain rates between 1 to 150 mm h^{-1}. The disdrometer data consists of measurements of N(D) in discrete intervals of ΔD at 30 seconds intervals which are subsequently averaged over 2 minutes. While several methods are available to fit the measured N(D) to a gamma form (e.g., Willis 1984), the method used here is based on Bringi and Chandrasekar (2001).

Once the set of (N_w, D_0, μ) parameters are obtained, the radar observables Z_h, Z_{dr} and K_{dp} are simulated based on the following assumptions:

1) Axis ratio versus D relation based on the fit proposed by Andsager et al. (1999).
2) Gaussian canting angle distribution with mean of 0^o and standard deviation 10°.
3) Truncation of the gamma DSD at D_{max}=3.5 D_m.

The simulated set of radar observables (Z_h, Z_{dr} and K_{dp}) when used in (23) gives an "effective" β of 0.0475 (for comparison the equilibrium β is 0.062).

Note that the algorithms for D_0 and N_w are constructed to be insensitive to the actual value of β, so that the details of the assumptions used in simulating the set of radar observables are not of particular relevance, and this fact is indeed the power of the proposed D_0 and N_w algorithms. In order to evaluate these algorithms using disdrometer measurements, the simulated values of Z_h, Z_{dr} and K_{dp} are used to calculate $\hat{D}_0$, $\hat{N}_w$ and $\hat{\mu}$ which are then compared against D_0, N_w and μ estimated by gamma fits to the set of measured N(D). Figure 7a shows the D_0 comparisons while Fig. 7b shows the NSD. Note that the $\hat{D}_0$ algorithm can retrieve the "true" D_0 quite accurately (NSD<7%) especially for D_0 > 1 mm. As expected the D_0 estimates get very accurate for higher values. The $\log_{10}$ (N_w) comparison are shown in Fig. 8a while 8b shows the NSD. The scatter in Fig. 8a shows that the accuracy in the retrieval of $\log_{10} N_w$ is quite high (<5 %) for N_w>1000 mm^{-1} m^{-3} (for reference the Marshall-Palmer value for N_w is 8000 mm^{-1} m^{-3}).

7. SUMMARY AND CONCLUSION

One of the long-standing goals of polarimetric radar has been the estimation of the parameters of the raindrop size distribution. Estimators for the parameters of a three parameter gamma model, namely D_0, N_w and μ are developed in this paper based on the radar observations Z_h, Z_{dr} and K_{dp}. The behavior of the three radar observations Z_h, Z_{dr} and K_{dp} are influenced by the underlying DSD, and the mean shape of raindrops. Z_{dr} is proportional to the reflectivity weighted axis ratio whereas K_{dp} is proportional to the volume weighted deviation of the axis ratio from unity. In addition, reflectivity is proportional to the sixth moment of the DSD, with corresponding variability due to polarization. Thus, the different polarimetric radar observations weight the DSD differently. It should be noted that the DSD estimates computed here correspond to radar measurements from the radar resolution volume. Among the three measurements (Z_h, Z_{dr} and K_{dp}), Z_{dr} is the most directly related to a parameter of the DSD, namely D_0. Gorgucci et al. (2000) described a procedure to estimate the mean shape-size relation of raindrops based on a simple linear model. Therefore, after the prevailing shape-size relation is established, Z_{dr} can be used to estimate D_0 directly. This concept is implemented in this paper as an algorithm to estimate D_0 from Z_h, Z_{dr} and K_{dp}. Statistical analysis of the estimator of D_0 indicates that it can be estimated to an accuracy of 10% when D_0 is 2 mm (and similar accuracies at the other D_0 values). Once D_0 is estimated, other measurements such as Z_h or K_{dp} can be used to estimate N_w, to a normalized standard deviation of about 6.5 % when N_w=8000 mm^{-1} m^{-3} and similar order at the other values. The estimation of μ is not easy because of the least influence of this parameter on the three measurements Z_h, Z_{dr} and K_{dp}. Therefore, the parametric estimates of μ derived are not as accurate. Measurement errors in Z_h, Z_{dr} and K_{dp} play a key role in the final accuracy of DSD estimates. Z_{dr} is a differential power measurement between two correlated signals, and can be measured accurately.

This high degree of accuracy in Z_{dr} translates to high accuracy in D_0. However, to estimate the prevailing mean shape-size relation, K_{dp} is needed which is relatively noisy at low rain rates. A hybrid approach is implemented in this paper such that when $K_{dp} \leq 0.2$ deg. km^{-1} the equilibrium shape model is used to estimate D_0. Bringi et al. (2002) have extended this procedure to low rain rates. The algorithms developed here were applied to one rainy season of disdrometer data collected in Darwin, Australia. The disdrometer analysis indicates that the algorithms work fairly well for the estimation of D_0 and N_w. In summary, the algorithms presented in this paper can be used to estimate the parameters of the raindrop size distribution, from polarimetric radar data at a frequency near 3 GHz (S-band), directly. However attenuation correction needs to be introduced for C and X band.

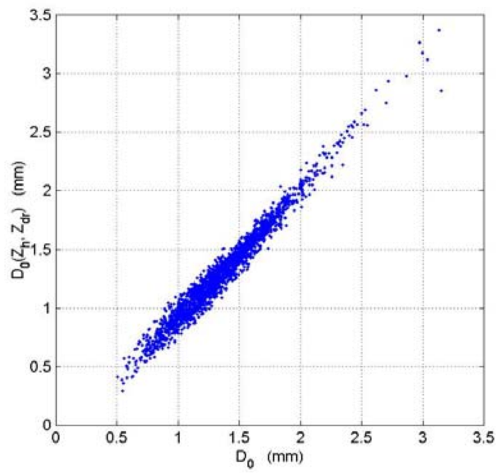

Figure 7a. Scatterplot of the estimate of D_0 computed from simulations of Z_h, Z_{dr} and K_{dp}, versus the direct estimate of D_0 for RSD obtained from a disdrometer located near Darwin, Australia.

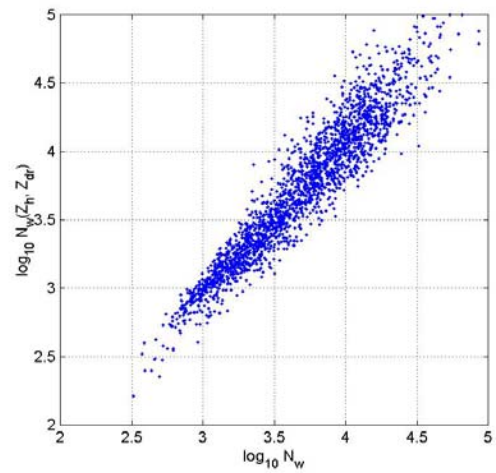

Figure 8a Scatterplot of $\log_{10} N_w(Z_h, Z_{dr})$, versus the direct estimate of $\log_{10} N_w$ for RSD obtained from a disdrometer located near Darwin, Australia.

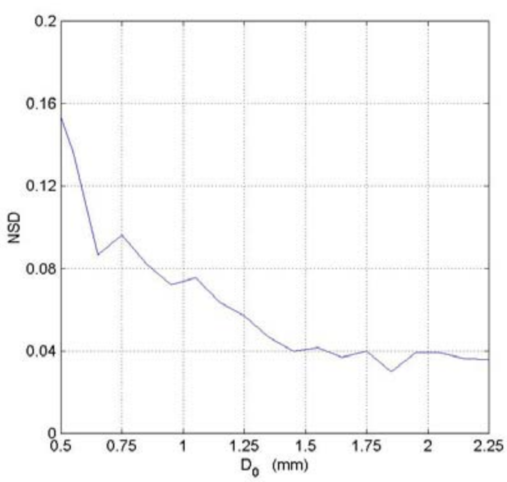

Figure 7b. Normalized standard deviation in the estimate of D_0, computed from simulations of Z_h, Z_{dr} and K_{dp}, versus the direct estimate of D_0 for RSD obtained from a disdrometer located near Darwin, Australia.

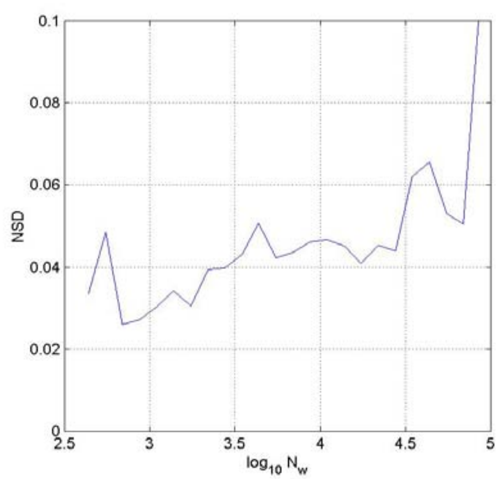

Figure 8b. Normalized standard deviation of $\log_{10} N_w(Z_h, Z_{dr})$, versus the direct estimate of $\log_{10} N_w$ for RSD obtained from a disdrometer located near Darwin, Australia.

8. ACKNOWLEDGEMENTS

Two of the authors (VC and VNB) acknowledge support from the NASA TRMM program. This research was supported partially by the National Group for Defense from Hydrological Hazard (CNR, Italy) and by the Italian Space Agency (ASI). The disdrometer data were provided by Dr. T. Keenan of the Bureau of Meteorology Research Center.

9. REFERENCES

Andsager, K., K. V. Beard and N. F. Laird, 1999: Laboratory measurements of axis ratios for large raindrops. *J. Atmos. Sci.*, **56**, 2673-2683.

Aydin, K., H. Direskeneli, and T. A. Seliga, 1987: Dual-polarization radar estimation of rainfall parameters compared with ground-based disdrometer measurements: October 29, 1982, Central Illinois experiment. *IEEE Trans. Geosci. Remote Sens.*, **GE-25**, 834-844.

Beard, K. V., and C. Chuang, 1987: A new model for the equilibrium shape of raindrops. *J. Atmos. Sci.,* **44,** 1509-1524.

Bringi, V. N., V. Chandrasekar, and R. Xiao, 1998: Raindrop axis ratio and size distributions in Florida rainshafts: an assessment of multiparameter radar algorithms. *IEEE Trans. Geosci. Remote Sensing*, **36**, 703-715.

Bringi, V. N. and V. Chandrasekar, 2001: Polarimetric Doppler Weather Radar: Principles and Applications. *Cambridge University Press ,* 636.

Bringi, V. N., Gwo-Jong Huang, V. Chandrasekar, and E. Gorgucci, 2002: A Methodology for estimating the parameters of a gamma raindrop size distribution model from polarimetric radar data: application to a squall-line event from the TRMM/Brazil campaign. *J. Atmos. Sci.*, (in press).

Chandrasekar, V., V. N. Bringi, and P. J. Brockwell, 1986: Statistical properties of dual polarized radar signals. Preprints, *23rd Conf. on Radar Meteorology*, Snowmass, CO, Amer. Meteor. Soc., 154-157.

Gorgucci, E., G. Scarchilli, and V. Chandrasekar, 1999: Specific differential phase shift estimation in the presence of non-uniform rainfall medium along the path. *J. Atmos. Oceanic Technol.*, **16**, 1690-1697.

Gorgucci, E., G. Scarchilli, and V. Chandrasekar, 2000: Measurement of mean raindrop shape from polarimetric radar observations. *J. Atmos. Sci.,* **57,** 3406-3413.

Gunn, R. and G. D. Kinzer, 1949: The terminal velocity of fall for water droplets in stagnant air. *J. Meteor.,* **6,** 243-248.

Hendry, A., Y. M. M. Antar, and G. C. McCormick, 1987: On the relationship between the degree of preferred orientation in precipitation and dual polarization radar echo characteristics. *Radio Sci.*, **22**, 37-50.

Jameson, A. R., 1985: Microphysical interpretation of multiparameter radar measurements in rain. Part III: Interpretation and measurement of propagation differential phase shift between orthogonal linear polarizations. *J. Atmos. Sci.,* **42,** 607-614.

Joss, J. and A. Waldvogel, 1967: A raindrop spectrograph with automatic analysis. *Pure Appl. Geophys.,* **68**, 240-246

Pruppacher, H. R and K. V. Beard, 1970: A wind tunnel investigation of the internal circulation and shape of water drops falling at terminal velocity in air. *Quart. J. Roy. Meteor. Soc.,* **96,** 247-256.

Sekhon R. S., and R. C. Srivastava, 1971: Doppler radar observations of drop-size distributions in a thunderstorm. *J. Atmos. Sci.*, **28**, 983-994.

Seliga, T.A., and V.N. Bringi, 1976: Potential use of the radar reflectivity at orthogonal polarizations for measuring precipitation. *J. Appl. Meteor.,* **15,** 69-76.

Testud J., E. L. Bouar, E. Obligis, and M. Ali-Mehenni, 2000: The rain profiling algorithm applied to polarimetric weather radar. *J. Atmos. Oceanic Technol.*, **17**, 332-356.

Ulbrich, C. W., 1983: Natural variations in the analytical form of raindrop size distributions. *J. Climate Appl. Meteor.,* **22**, 1764-1775.

Willis, P. T., 1984: Functional fits to some observed drop size distribution and parameterization of rain. *J. Atmos. Sci.*, **41**, 1648-1661.